DOI: 10.1002/ejoc.200900837

Synthesis and Stereochemical Properties of "Extended" Biphenols Bridged by *ortho*-, *meta*-, and *para*-Phenylene Spacers

Mariusz M. Gruza,[a] Jean-Claude Chambron,*[a] Enrique Espinosa,*[b] and Emmanuel Aubert[b]

Keywords: Cross-coupling / Biaryls / Atropisomerism / Density functional calculations

A series of isomeric biphenols based on *para*- (**1**), *meta*- (**2**), and *ortho*- (**3**) terphenyl backbones was synthesized. Suzuki cross-coupling methodology was employed for the construction of the terphenyl backbone of their methyl-protected precursors (respectively **8**, **13**, and **16**). Using K_2CO_3 as the base, the best reaction conditions involved DMF at 100 °C as solvent. Anhydrous conditions greatly improved the yields of the sterically crowded systems (particularly **16**). *ortho*-Terphenyls **3** and **16** exist as mixtures of *syn*/*anti* atropisomers in solution. Compound **16** crystallizes in the *anti-in* form. DFT calculations at the B3LYP/6-311+G(d,p) level indicate that for both compounds the *anti-in* form is more stable than the *syn* form by 6.07 and 2.07 kJ mol^{-1} for **16** and **3**, respectively. These $\Delta\Delta G^0$ values are higher by the same factor (of two) than those obtained in solution at 240 K (3.17 and 0.93 kJ mol^{-1}). The atropisomeric properties of **16** and **3** are finally discussed in the context of *ortho*-terphenyls in the literature.

Introduction

Biphenols, especially those derived from 1,1′-biphenyl-2,2′-diol and BINOL, are very important ligands (in the deprotonated form) and precursors of ligands (phosphites, phosphoamidites, and phosphanes) that are involved in a variety of transition-metal-catalyzed reactions.[1] We found a very efficient preparation of biphenol **1** (Figure 1) via its methyl ether precursor by a double Suzuki coupling reaction in DMF. Because of the 1,4-phenylene bridge, deprotonation of biphenol **1** cannot generate a chelate. However, this is not the case of isomeric biphenols **2** and **3**, which contain 1,3- and 1,2-phenylene spacers, and they could form 10- and 9-membered chelate rings, respectively, in their metal complex derivatives.

Noteworthy, biphenol **2** was recently shown to act as an $[OCO]^{3-}$ trianionic pincer ligand in Ta^{V} and $Mo^{IV/VI}$ complexes:[2,3] for example, reaction of **2** with $Mo(NMe_2)_4$ led to C–H bond activation and produced the C_s-symmetric octahedral Mo^{IV} complex *mer*-[Mo(**2**-3 H)$(NHMe_2)_2(NMe_2)$], from which a reactive nucleophilic Mo^{VI} nitrido complex could be prepared. The protected form of **2** had been previously obtained in 57% yield by using the procedure of Hart and co-workers, who developed an efficient synthesis of various *meta*-terphenyl derivatives from 2,6-dibromoiodobenzene and aryl Grignard reagents.[4]

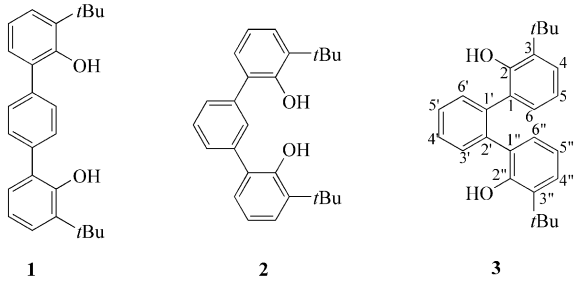

Figure 1. Chemical structures of biphenols **1**–**3**.

These recent remarkable findings prompted us to report the preparation of biphenols **1**–**3** by double Suzuki coupling of easy-to-access precursors. This work also presents a study of the compared stereochemical properties of the new members of the series, biphenol **3** and its methylated precursor, **16**.

Results and Discussion

Synthesis

The four-step synthesis of biphenol **1** is shown in Scheme 1. 2-Bromo-6-*tert*-butylphenol (**5**) was obtained as described in the literature, by bromination of 2-*tert*-bu-

[a] ICMUB (CNRS UMR 5260), Université de Bourgogne, 9 avenue Alain Savary, 21078 Dijon, France
Fax: +33-3-80396117
E-mail: jean-claude.chambron@u-bourgogne.fr
[b] CRM2 (CNRS UMR 7036), Institut Jean Barriol, Nancy-Université,
Boulevard des Aiguillettes, 54506 Vandœuvre-lès-Nancy, France
Fax: +33-3-83406492
E-mail: enrique.espinosa@crm2.uhp-nancy.fr
Supporting information for this article is available on the WWW under http://dx.doi.org/10.1002/ejoc.200900837.

tylphenol (**4**) with Me_2NBr prepared in situ.[5] It was converted quantitatively into 1-bromo-3-*tert*-butyl-2-methoxybenzene (**6**) by methylation with CH_3I in the presence of KOH as base in THF. Terphenyl **8** was prepared through double Suzuki coupling of bromoanisole derivative **6** with commercially available diboronic acid **7**, using the "classical reagents" $[Pd(PPh_3)_4]$ as catalyst (2.7 mol-%) and *aqueous* K_2CO_3 as base.[6] Initial attempts involved either refluxing DME or toluene as solvents, affording terphenyl **8** in only 39 and 56% yield, respectively. However, when the solvent was changed to DMF (at 100 °C), the yield of the reaction was considerably improved (98%).[7] Finally, demethylation by using standard conditions (BBr_3, CH_2Cl_2, 0 °C) afforded diphenol **1** in 90% yield. Interestingly, this compound was first reported as a minor product (9%) of the catalytic *ortho*-arylation of 2-*tert*-butylphenol (ArOH) with unsymmetrical aryl dihalide 4-chloro-1-bromobenzene by $[RhCl(PPh_3)_3]$/P*i*Pr$_2$(OAr), a reaction that produced mainly (26%) 3-*tert*-butyl-4′-chloro-biphenyl-2-ol.[8]

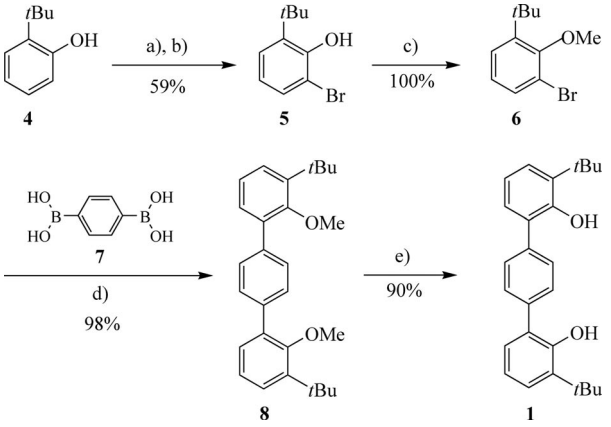

Scheme 1. Reagents and conditions: (a) Br_2, Me_2NH; (b) PhMe, –15 °C; (c) KOH (3.3 equiv.), MeI (3.6 equiv.), THF, reflux; (d) $[Pd(PPh_3)_4]$ (2.7 mol-%), K_2CO_3 (4.5 equiv.), DMF/H_2O, 100 °C; (e) BBr_3 (2.5 equiv.), CH_2Cl_2, 0 °C.

The preparation of diphenols **2** and **3** involved boronic acid **10** and commercially available 1,3- and 1,2-dibromobenzene (**11**) and (**14**), respectively, as reactants in double Suzuki coupling reactions. At first, reaction of **4** with KOH/MeI afforded anisole derivative **9** in 97% yield, which was subsequently converted into 3-*tert*-butyl-2-methoxyphenylboronic acid (**10**) by *ortho*-lithiation followed by quenching of the organolithium derivative with B(O*i*Pr)$_3$ and HCl hydrolysis.[9] Compound **10** was isolated in 65% yield after purification (Scheme 2).

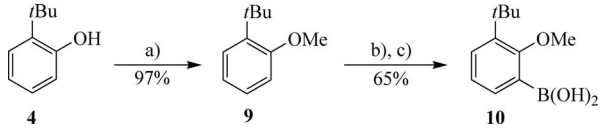

Scheme 2. Reagents and conditions: (a) NaH, MeI, THF; (b) *n*BuLi/TMEDA (1.5 equiv.), B(O*i*Pr)$_3$ (2 equiv.), THF; (c) 5% aq. HCl.

Double Suzuki coupling of boronic acid **10** with 20% excess of 1,3-dibromobenzene (**11**) under similar conditions {2.4 mol-% $[Pd(PPh_3)_4]$, *aqueous* K_2CO_3, DMF, 100 °C} produced the monosubstituted biphenyl **12** mainly, alongside with desired terphenyl **13** (Scheme 3, conditions a). For example, after 12 h reaction time these compounds were isolated in 70 and 30% yield, respectively. Extension of the reaction time to 3 d allowed **12** and **13** to be isolated in 59 and 41% yield, respectively. Noticeably, reaction mixtures darkened quickly, indicating catalyst decomposition. Fortunately, this could be minimized by working under *anhydrous* conditions, as previously observed in the case of sterically hindered substrates.[10] At 3 mol-% loading of catalyst, 4 d reaction time and 50% excess of **11**, the reaction was driven to the formation of terphenyl **13** as the major product (59% yield); biphenyl **12** was obtained in 11% yield only (Scheme 3, conditions b).[11]

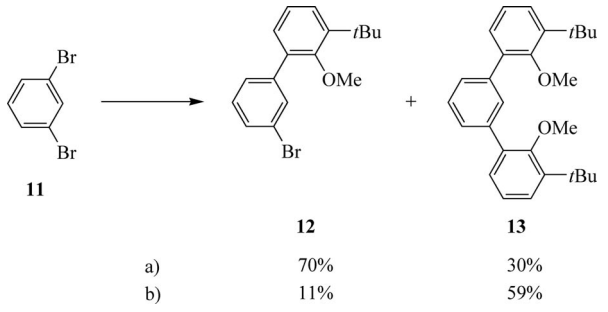

Scheme 3. Reagents and conditions: (a) **10** (1.73 equiv.), $[Pd(PPh_3)_4]$ (2.4 mol-%), K_2CO_3 (3.5 equiv.), DMF/H_2O (9:1), 100 °C; (b) **10** (3 equiv.), $[Pd(PPh_3)_4]$ (3 mol-%), K_2CO_3 (4.5 equiv.), DMF, 100 °C.

Double Suzuki coupling of boronic acid **10** with 1,2-dibromobenzene (**14**) under anhydrous reaction conditions ($[Pd(PPh_3)_4]$, K_2CO_3, DMF, 100 °C) worked slightly better: target terphenyl **16** was isolated in 64% yield, and the formation of biphenyl **15** was not observed (Scheme 4, conditions a). Interestingly, the course of the reaction could be stopped to the selective and quantitative formation (98%) of biphenyl **15** by changing DMF to ether solvents (DME or THF) in a "wet" reaction system. In agreement with the

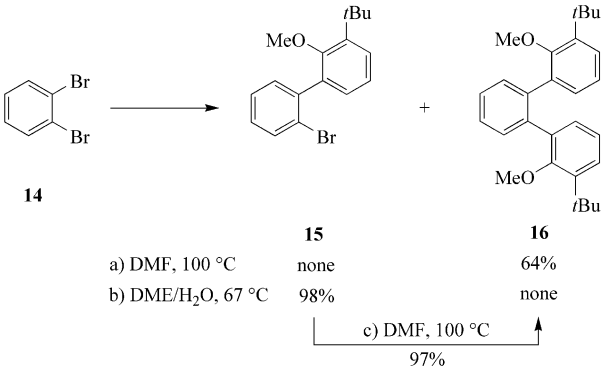

Scheme 4. Reagents and conditions: (a) **10** (2.88 equiv.), $[Pd(PPh_3)_4]$ (2.1 mol-%), K_2CO_3 (4 equiv.); (b) **10** (3.7 equiv.), $[Pd(PPh_3)_4]$ (2.7 mol-%), K_2CO_3 (4.2 equiv.); (c) **10** (4 equiv.), $[Pd(PPh_3)_4]$ (10 mol-%), K_2CO_3 (6 equiv.), DMF, 100 °C.

previous observations, Suzuki coupling of intermediate bromodiphenyl **15** with boronic acid **10** under *anhydrous* reaction conditions ([$Pd(PPh_3)_4$], K_2CO_3, DMF, 100 °C) afforded desired terphenyl **16** in high yield (97%). Therefore, the best preparation of **16** is a sequence of two single Suzuki coupling reactions (in different solvents) involving **15** as the intermediate. The overall yield is 95% (Scheme 4, conditions b,c).

Cleavage of the methoxy groups (BBr_3, CH_2Cl_2, –78 °C) afforded diphenols **2** and **3** in 54 and 78% isolated yield, respectively.

Stereochemical Properties of *o*-Terphenyls 3 and 16

Biphenol **3** and its direct precursor **16** belong to the family of *ortho*-terphenyls. Conformational analysis of *ortho*-terphenyl derivatives can be described as illustrated in Figures 2 and 3.[12] These compounds show two basic average conformations, chiral (C_2 symmetric) *anti* and achiral (C_s symmetric) *syn*, depending on the mutual orientations of the largest (R) substituents with respect to the plane of the central phenyl fragment. Exchange between these forms results from rotation about the phenyl–phenyl C–C bonds. In addition, oscillation motions determine limiting forms, which are enantiomeric and degenerate in the case of the *syn* conformation, and diastereomeric in the case of the *anti* conformation, that is, *anti-in* and *anti-out*, depending on the position of the R substituent with respect to the C_2 symmetry axis of the molecule: remote (*out*) or close (*in*).

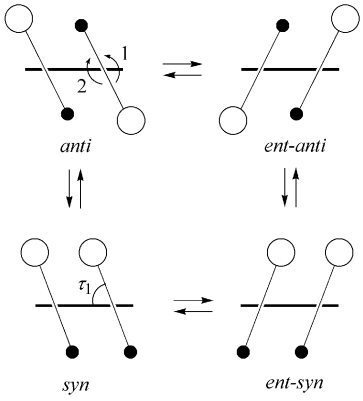

Figure 2. The *anti* and *syn* conformations of *ortho*-terphenyls. The empty disk represents the largest (R) substituent. Curved arrows represent the two possible pathways for the *anti*/*syn* interconversion.

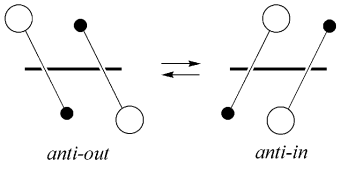

Figure 3. The *anti-in* and *anti-out* conformations of *ortho*-terphenyls. The empty disk represents the largest (R) substituent.

DFT computations [B3LYP/6-311+G(d,p) level] of **16** show that, in addition to the anticipated three energy minimum conformations of Figures 2 and 3 (*anti-in*, *anti-out*, and *syn*), there is an additional energy minimum *anti* conformation (*anti-in*,*out*), which arises from atropisomerism about the C_{phenyl}–O bond (Supporting Information, Figure S2). The most and least stable atropisomers are the *anti-in* ($\Delta G^0 = 0$) and *syn* ($\Delta G^0 = +6.07$ kJ mol^{-1}) conformation, respectively. The *anti-in*,*out* ($\Delta G^0 = +3.65$ kJ mol^{-1}) and *anti-out* ($\Delta G^0 = +4.20$ kJ mol^{-1}) conformations show intermediate relative energies. These data are collected in Table 1 together with the computed torsion angles τ_1 and τ_2 (Supporting Information, Figure S1) around the central C_{phenyl}–C_{phenyl} and C_{phenyl}–O bonds, respectively.

Table 1. Standard free energies and characteristic torsion angles for the conformers of **16** and **3**.

Rotamer	ΔG^0 [kJ mol^{-1}][a]	τ_1 [°][b]	τ_2 [°][b]
16 *anti-in*	0	+64.3/+64.3	+67.5/+67.5
16 *anti-in*,*out*	+3.65	+87.8/+122.6	+66.1/–65.6
16 *anti-out*	+4.20	+130.0/+130.0	–66.0/–66.0
16 *syn*	+6.07	+68.6/–134.1	+70.7/+64.7
3 *anti-in*	0	+74.8/+74.8	+0.1/+0.1
3 *anti-out*	+0.36	+113.3/+113.3	+1.8/+1.8
3 *syn*	+2.07	–120.2/+72.0	–8.0/+0.3

[a] Gas-phase standard free energy differences with respect to the *anti-in* conformation. [b] See Figure S1 (Supporting Information).

Single-crystal X-ray diffraction shows that **16** has also the most stable computed *anti-in* conformation in the solid state (Figure 4). The measured torsion angles (60.1 and 61.3°) match approximately the calculated ones (64.3 and 67.5°, respectively; Table 1).

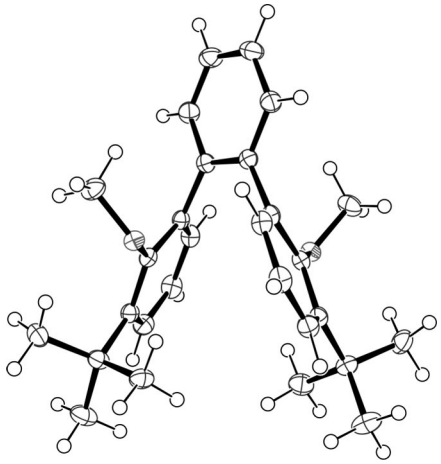

Figure 4. ORTEP view of the X-ray crystal structure of *ortho*-terphenyl **16**. Ellipsoids are drawn at the 50% probability level.

The results of the conformational analysis carried out by DFT are summarized in Figure 5, in which the calculated conformers (Supporting Information, Figure S2) and transition states (Supporting Information, Figure S3) are schematically depicted along with their relative standard free energies. Interconversion barriers as well as structural data for the transition states are collected in Table 2. Starting from the lowest energy *anti-in* conformation, the intermedi-

ate asymmetric *anti-in*,*out* conformation is obtained by torsion about one of the C_{phenyl}–O bonds, which affects the τ_1 angles. The energy barrier of this process is 21.45 kJ mol^{-1}. Similarly, the transition from *anti-in*,*out* to the higher energy *anti-out* conformation involves torsion about the other C_{phenyl}–O bond, with a slightly lower energy barrier (17.38 kJ mol^{-1}). The *anti-in* to *syn* conversion may occur by either of two possible pathways, depending on the sense of rotation of one of the C_{phenyl}–C_{phenyl} bonds relative to the other (Figure 2). In pathway 1, the rotation moves the methoxy and *t*Bu substituents away from the central phenylene ring, whereas in pathway 2 it brings these substituents towards the central ring. Strain arises when the rotating and the central aromatic rings become coplanar. In the first case, steric repulsion between the methoxy group and a hydrogen atom of the central phenylene ring is minimized by gearing of the methoxy group inside the adjacent *t*Bu. The energy barrier corresponding to this process is 76.02 kJ mol^{-1}. Transfer of the methoxy group to the opposite side of the phenylene ring leaves the *t*Bu substituent rotated by 60° relative to its initial orientation. The lowest energy *syn* conformation is finally obtained by rotation of *t*Bu back to its initial position; the energy barrier of this latter process is negligible. In the second case, rotation about the C_{phenyl}–C_{phenyl} bond again induces gearing of the methoxy group inside the *t*Bu substituent, along with a reorientation of the other methoxy group. The corresponding transition state has an activation free energy of 113.03 kJ mol^{-1}. Further rotation of the first methoxy group to reach the final *syn* conformation involves a second transition state with a lower energy barrier (40.70 kJ mol^{-1}). The conversion of the *anti-in* to the *syn* form is significantly easier along the first pathway. Indeed, the corresponding transition state involves a C–H···O hydrogen bond (1.98 Å, 128.69°) and a C–H···π interaction (2.31 Å, 157.87°), which have no equivalent in the other transition states (Supporting Information, Figure S3).

The results of the conformational analysis carried out by DFT for **3** are summarized in Figure 6, in which the calculated conformers (Supporting Information, Figure S4) and transition states (Supporting Information, Figure S5) are schematically depicted along with their relative standard free energies. In comparison to **16**, the case of **3** is simpler, owing to the fact that the hydroxy group has less rotational freedom than the methoxy group. The three expected energy minima are thus also found by DFT calculations (Table 1; Figure 7; Supporting Information, Figure S4): the lowest, the highest, and the intermediate energy minima correspond, respectively, to the *anti-in* ($\Delta G^0 = 0$), *syn* ($\Delta G^0 = +2.07$ kJ mol^{-1}), and *anti-out* ($\Delta G^0 = +0.36$ kJ mol^{-1}) conformations. Hence, contrary to the case of **16**, **3** shows very little preference for *anti-in* over *anti-out*. This could result from the fact that both conformers are stabilized by very similar O–H···π interactions, exhibiting equivalent distances (2.29 Å). The *anti-in* to *anti-out* conversion is an easy process, as its barrier is only 6.67 kJ mol^{-1} (Supporting Information, Figure S5). This is not the case for the *anti* to *syn* conversion, which can follow either of the two processes

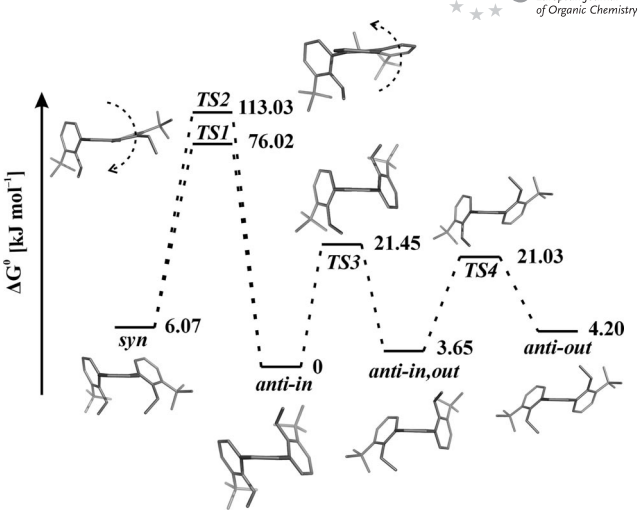

Figure 5. Energy profile for the interconversion between the *syn*, *anti-in*, and *anti-out* conformers of **16** (standard free energy in kJ mol^{-1}). Transition states are denoted by TS1 (*anti-in*/*syn*-1), TS2 (*anti-in*/*syn*-2), TS3 (*anti-in*/*anti-in,out*), and TS4 (*anti-in,out*/*anti-out*). For TS1 and TS2 involved in the interconversion from *anti-in* to *syn* conformers, the curved arrows indicate the rotation of one phenyl group bearing OMe and *t*Bu substituents relative to the central ring.

Table 2. Standard free energies and torsion angles of the transition states.

Transition state	$\Delta G^{0‡}$ [kJ mol^{-1}][a]	τ_1 [°][b]	τ_2 [°][b]
16 *anti-in*/*syn*-1	+76.02	+90.1/+164.6	+64.4/+89.0
16 *anti-in*/*syn*-2	+113.03	–13.4/+72.8	+81.2/+66.3
16 *anti-in*/*anti-in,out*	+21.45	+73.3/+95.3	+67.8/–5.2
16 *anti-in,out*/*anti-out*	+17.38	+109.1/+130.3	–0.2/–66.4
3 *anti-in*/*syn*-1	+76.81	+73.4/–172.6	+0.6/–50.8
3 *anti-in*/*syn*-2	+79.24	+87.8/–1.8	+3.4/+3.1
3 *anti-in*/*anti-out*	+6.67	+82.5/+82.5	+2.0/+2.0

[a] Gas-phase standard activation free energy. [b] See Figure S1 (Supporting Information).

identified for **16**. In the first one, the hydroxy group is placed in a perpendicular orientation with respect to the rotating phenyl ring. The corresponding transition state has a standard free-activation energy of 76.81 kJ mol^{-1} and is characterized by the setting up of a C–H···O hydrogen bond (2.07 Å, 125.6°) and a C–H···π interaction (2.16 Å, 126.8°). Passing through this barrier a stable intermediate is reached, the OH proton being locked into the adjacent *t*Bu group. However, the activation energy required to pass over the barrier separating this intermediate from the more stable *syn* conformation is only 6.44 kJ mol^{-1}. The second process involves only one transition state, which is 79.24 kJ mol^{-1} higher in energy than the *anti-in* conformation and is characterized by short O–H···π (1.80 Å, 166.5°) and H···H (1.63 Å) interactions.

Whereas the room-temperature ^{1}H NMR spectra of *meta*- and *para*-terphenyls **1**, **2**, **8**, and **13** all display well-resolved features, this is not the case for *ortho*-terphenyls **3** and **16**, which show broadened signals. Actually, two sets of signals can be clearly identified in the room-temperature spectrum of **16**. A stacked plot of its variable-temperature

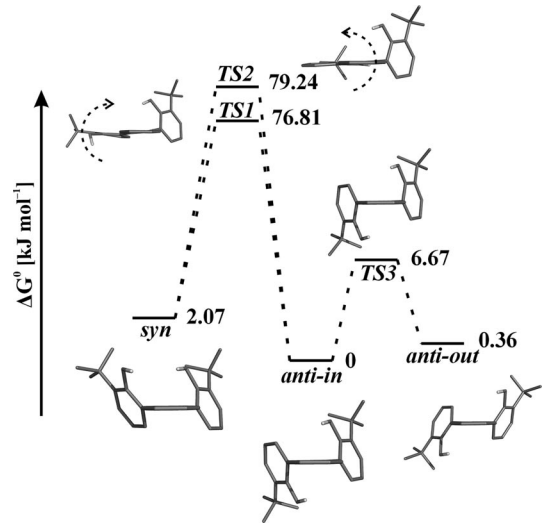

Figure 6. Energy profile for the interconversion between the *syn*, *anti-in*, and *anti-out* conformers of **3** (standard free energy in kJ mol^{-1}). Transition states are denoted by TS1 (*anti-in*/*syn*-1), TS2 (*anti-in*/*syn*-2), and TS3 (*anti-in*/*anti-out*). For TS1 and TS2, involved in the interconversion from *anti-in* to *syn* conformers, the curved arrows indicate the rotation of one phenyl group bearing OH and *t*Bu substituents relative to the central ring.

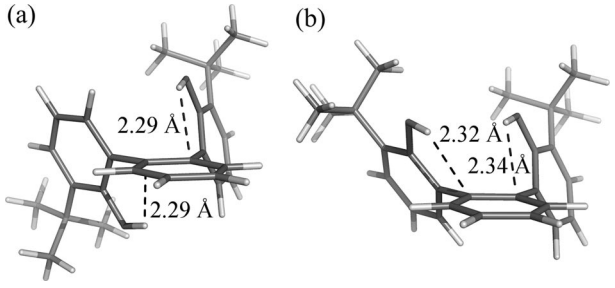

Figure 7. Optimized structures for the two conformers of **3** [B3LYP/6-311+G(d,p)]: (a) *anti-in* and (b) *syn*. OH···π interactions are shown with dashed lines.

(VT) ^{1}H NMR spectra in the temperature range 275–410 K in $C_2D_2Cl_4$ is presented in Figure 8. At 275 K, the two sets of peaks are well resolved, but most of them broaden upon heating. Coalescence for the methoxy and *tert*-butyl systems takes place at 330 and 315 K, respectively, whereas coalescence for the aromatic protons is noted at 300 (4,4′′), 315 (5,5′′), and 340 K (6,6′′). The ^{1}H NMR spectrum then gradually evolves to what is finally observed at 410 K, where only one set of well-resolved signals can be identified.

Terphenyl **16** indeed exists as a mixture of *syn* and *anti* stereoisomers, which do not interconvert at 275 K. The methoxy singlet of the major isomer is shifted upfield by 0.29 ppm with respect to the corresponding signal of the minor isomer. This suggests that the former is the *anti* form, in which the methoxy (anisyl) groups are shielded. This assignment is confirmed by the 2D ROESY ^{1}H–^{1}H NMR spectrum, in which the same methoxy signal is correlated with the doublet of protons 6 and 6′′ (whereas the methoxy singlet of the minor isomer does not show such a correlation), a situation which can exist only in the *anti* atropisomer (Supporting Information, Figure S7). The ratio between the *anti* and *syn* forms is 80:20 at 275 K. This corresponds to a $\Delta\Delta G$ value of –3.17 kJ mol^{-1}. The VT ^{1}H NMR spectroscopic data of **16** were analyzed by the coalescence temperature (T_c) method, which allowed the free-activation energy for the *anti*/*syn* interconversion to be estimated as a function of temperature (Table 3).

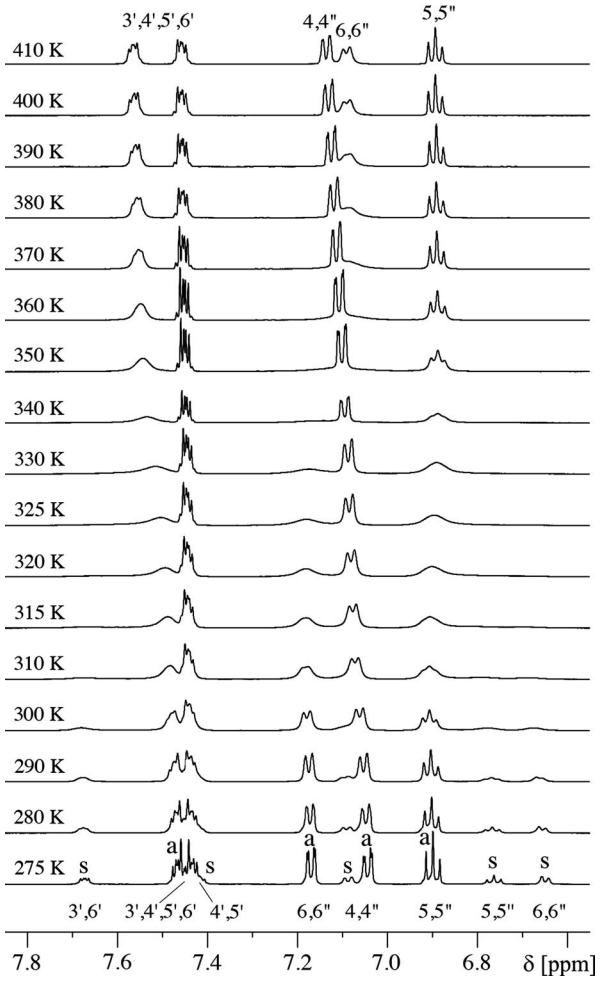

Figure 8. Stacked plot of the VT ^{1}H NMR spectra of terphenyl **16** in $C_2D_2Cl_4$ (aromatic region).

Similar behavior was observed in the case of biphenol **3** under the same conditions (Supporting Information, Figures S6 and S8). The distribution between the *anti* and *syn* forms is 58:42 at 240 K, and ca. 60:40 at 275 K. The corresponding $\Delta\Delta G$ value at this latter temperature is –0.93 kJ mol^{-1}, which can be directly compared to the –3.17 kJ mol^{-1} value obtained for compound **16**. Comparison of $\Delta G_c^{\ddagger}$ values at two identical temperatures (300 and 315 K) shows that the free-activation energies of **16** and **3** are very close to each other, the methyl substitution making $\Delta G_c^{\ddagger}$ higher by 1 kJ mol^{-1} only. This indicates that, in agreement with the DFT calculations, the *anti*/*syn* conversion takes place by process 1 rather than process 2 of Figure 2. This is also in keeping with the nearly equal effective van der Waals radii of OH (1.53 Å) and OCH_3 (1.52 Å).[12b]

Table 3. Observed coalescences and calculated free-activation energies from the VT ^{1}H NMR spectra of terphenyls **16** and **3** in $C_2D_2Cl_4$ at 500 MHz.

	Probe protons	^3J[a] [Hz]	T_c[b] [K]	$\Delta\nu$[c] [Hz]	$\Delta G_c^{\ddagger}$[d] [kJ mol^{-1}]
16	4,4′′	7.87	300	21.3	63.1
	5,5′′	7.65	315	65.3	64.2
	6,6′′	7.50	340	242.7	65.8
	OCH_3		330	141.6	65.3
	*t*Bu		315	64.4	64.3
3	4,4′′	7.85	280	8.7	59.5
	5,5′′	7.62	300	40.5	62.0
	6,6′′	7.48	315	91.0	63.3
	OH		325	128.7	64.5
	*t*Bu		300	35.5	62.6

[a] Averaged coupling constants at T = 240 K. [b] Coalescence temperature. [c] Frequency difference determined by extrapolation at T_c. [d] Calculated according to $\Delta G_c^{\ddagger} = RT_c[22.96 + \ln T_c - \ln(\Delta\nu^2 + 6J^2)^{1/2}]$.

Decreasing the temperature from 280 to 185 K (CD_2Cl_2) did not bring about significant changes in the ^{1}H NMR spectra of either **16** or **3**, except that in the latter case the OH signal of the *syn* diastereomer broadened and shifted downfield by 0.58 ppm, whereas in the same temperature range the OH signal of the *anti* diastereomer did not broaden significantly and shifted downfield by 0.14 ppm only. Actually, the fact that no coalescence phenomenon occurs in this temperature range is not surprising, as the computed maximal free-activation energies for the *anti-in* to *anti-in,out* (**16**) and for the *anti-in* to *anti-out* (**3**) transitions are, respectively, 21.45 and 6.67 kJ mol^{-1}, which correspond to theoretical coalescence temperatures of 111.2 and 35.5 K.[13] In other words, in the temperature range of our investigations, the *anti* form observed results from exchange of the *anti-in* and *anti-out* forms characterized by computation studies.

Comparison of the calculated and measured thermodynamic data for the *anti-in* to *syn* conversion of terphenyls **16** and **3** shows that the theoretical $\Delta\Delta G^0$ values (respectively, 6.07 and 2.07 kJ mol^{-1}) are higher by the same factor (of two) by comparison with those obtained at 275 K by VT NMR (3.17 and 0.93 kJ mol^{-1}, respectively), which points to the validity of the calculations. The same is true for the kinetic data. The calculated $\Delta G^{0\ddagger}$ values corresponding to the *anti*/*syn*-1 transition are very close to each other (76.02 and 76.81 kJ mol^{-1} for **16** and **3**, respectively), as are the $\Delta G_c^{\ddagger}$ values measured by VT NMR (Table 3).

The dynamic properties of various *ortho*-terphenyl derivatives (Figure 9) have been reported.[12] The corresponding data are collected in Table 4. Direct comparison of terphenyls **16** and **19** is possible, as the $\Delta G_c^{\ddagger}$ values are available at 330 K in both cases. The difference of –8.5 kJ mol^{-1} between the $\Delta G_c^{\ddagger}$ values of **16** and **19** shows that the (OCH_3, *t*Bu) pair of substituents (R, X) in the former is less sterically hindering than the corresponding pair (CH_3, Cl) in the latter. This seems at first paradoxical, as the buttressing effect of *t*Bu is expected to be much stronger than that of Cl, but it can be explained by the higher effective van der Waals radius of CH_3 (1.80 Å) by comparison with that of OCH_3 (1.52 Å).[12b] In addition, as shown by DFT calculations, gearing of the OCH_3 substituent inside the *t*Bu group provides a low-energy pathway for atropisomerization, which is not possible in **19**.

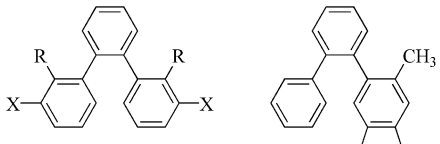

17: R = OCH_3, X = H
18: R = CH_3, X = H
19: R = CH_3, X = Cl
20: R = H, X = *i*Pr

21

Figure 9. Other *ortho*-terphenyls of the literature (see Table 4 for the references).

Table 4. Calculated free-activation energies for various *ortho*-terphenyls.

Compound[a]	R	X	T_c[b] [K]	$\Delta G_c^{\ddagger}$ [kJ mol^{-1}]	Ref.
3	OH	*t*Bu	300	62.0	this work
16	OCH_3	*t*Bu	300	63.1	this work
			330	65.3	this work
17	OCH_3	H	n.a.	n.a.	[12a]
18	CH_3	H	282	61.9	[12a]
19	CH_3	Cl	331	73.7	[12a]
20	H	*i*Pr		32.2	[12c]
21	–	–	302	70.5	[12b]

[a] See Figure 9. [b] Coalescence temperatures used to calculate $\Delta G_c^{\ddagger}$.

Conclusions

This work has presented the syntheses of a series of isomeric "biphenols" based on terphenyl backbones and phenylene spacers by Suzuki cross-coupling reactions. Except the *para* isomer, these compounds in their anionic form are either proven (i.e., **2**) or potential (i.e., **3**) chelate biphenolate ligands. The latter (i.e., **3**) as its methylated precursor **16**, exists as a mixture of *anti* (major) and *syn* (minor) atropisomers at low temperature (down to 185 K). The experimental (^{1}H NMR) barriers for the *anti*/*syn* transition are virtually the same for both compounds (62.0 and 63.1 kJ mol^{-1}, respectively, at 300 K). DFT calculations at the B3LYP/6-311+G(d,p) level of theory give a value that is ca. 13 kJ mol^{-1} higher, but similar barriers and predict that the *anti* form of **3** and **16** has two energy minima, the most stable *anti-in* and the least stable *anti-out*. In addition, an intermediate situation (*anti-in,out*) is also theoretically calculated for **16**. However, these conformations could not be evidenced experimentally. Indeed, they are separated by relatively low energy barriers (<21.5 kJ mol^{-1}), being predicted to show up at temperatures less than ca. 110 K only.

Experimental Section

General Information: 2-Bromo-6-*tert*-butylphenol (**5**)[5] was prepared according to the literature. Unless otherwise stated, all reactions were performed under an atmosphere of argon by using standard Schlenk techniques. Dimethylformamide was filtered through alumina and stored over molecular sieves; THF was distilled from sodium/benzophenone and dichloromethane over phosphorus pentoxide. All other chemicals were used as received. NMR spectra were obtained by using a Bruker DRX 500 (500 MHz) spectrometer or a Bruker Avance (600 MHz) spectrometer. ^{1}H and ^{13}C NMR spectra were recorded at 500.13 or 600.13 MHz, and 125.76 MHz or 150.92 MHz, respectively. Assignments of the *syn* and *anti* isomers of terphenyls **16** and **3** were carried out at 278.5 and 273 K, respectively, using 2D ^{1}H–^{1}H ROESY, ^{13}C–^{1}H HSQC, and ^{13}C–^{1}H HMBC NMR spectroscopy. IR spectra were recorded with a Bruker IFS 66v Fourier transform IR spectrophotometer. Melting points were measured with a Büchi Melting Point B-545 apparatus. Elemental analyses were run with an EA1108 CHNS Fisons Instrument analyzer.

1-Bromo-3-*tert*-butyl-2-methoxybenzene (6): Freshly powdered KOH (4 g, 71.3 mmol) was added to a solution of **5** (5.0 g, 21.8 mmol) in THF (50 mL), and the resulting mixture was stirred for 30 min at room temperature. After dropwise addition of CH_3I (4.75 mL, 76.3 mmol) at 0 °C, the reaction mixture was stirred for 40 min at this temperature and overnight at room temperature. It was quenched with water (100 mL) and extracted with CH_2Cl_2 (4 × 50 mL). The combined organic extract was washed with water (50 mL) and brine (50 mL) and dried ($MgSO_4$). Column chromatography (alumina; heptane/CH_2Cl_2, 95:5) afforded **6** (5.41 g) as an oil that solidified upon standing. Yield: 99.9%. M.p. 45–46 °C.^{1}H NMR (500 MHz, $CDCl_3$): δ = 7.42 (dd, $^4J_{H,H}$ = 1.6 Hz, $^3J_{H,H}$ = 7.9 Hz, 1 H, 4-H or 6-H), 7.27 (dd, $^4J_{H,H}$ = 1.6 Hz, $^3J_{H,H}$ = 7.9 Hz, 1 H, 6-H or 4-H), 6.89 (t, $^3J_{H,H}$ = 7.9 Hz, 1 H, 5-H), 3.93 (s, 3 H, OCH_3), 1.39 (s, 9 H, *t*Bu-H) ppm. ^{13}C NMR (125 MHz, $CDCl_3$): δ = 156.7, 145.3, 132.1, 126.4, 124.5, 118.1, 61.4, 35.5, 30.9 ppm. $C_{11}H_{15}BrO$ (243.14): calcd. C 54.34, H 6.22; found C 54.03, H 6.19.

3,3′′-Di-*tert*-butyl-2,2′′-dimethoxy[1,1′;4′,1′′]terphenyl (8): $[Pd(PPh_3)_4]$ (0.256 g, 0.22 mmol) and K_2CO_3 (5.13 g, 37.2 mmol) in water (8 mL) were added to a solution of **6** (4.40 g, 18.12 mmol) and diboronic acid **7** (1.37 g, 8.26 mmol) in DMF (100 mL). The reaction mixture was heated to 100 °C for 20 h under vigorous stirring. Addition of water precipitated a white solid that was collected by filtration. The mother liquor was extracted with CH_2Cl_2 (3 × 100 mL). Column chromatography (silica; heptane/CH_2Cl_2, 85:15) of the crude product afforded **8** (3.256 g) as a colorless solid. Yield: 98%. M.p. 167–170 °C. ^{1}H NMR (500 MHz, $CDCl_3$): δ = 7.63 (s, 4 H, 2′-H, 3′-H, 5′-H and 6′-H), 7.34 (dd, $^3J_{H,H}$ = 7.7 Hz, $^4J_{H,H}$ = 1.7 Hz, 2 H, 4,4′′-H), 7.25 (dd, $^3J_{H,H}$ = 7.7 Hz, $^4J_{H,H}$ = 1.7 Hz, 2 H, 6,6′′-H), 7.10 (t, $^3J_{H,H}$ = 7.7 Hz, 2 H, 5,5′′-H), 3.36 (s, 6 H, OCH_3), 1.46 (s, 18 H, *t*Bu-H) ppm. ^{13}C NMR (125 MHz, $CDCl_3$): δ = 157.8, 143.2, 138.8, 135.2, 129.9, 129.2, 126.6, 123.3, 60.5, 35.3, 31.0 ppm. $C_{28}H_{34}O_2$ (402.576): calcd. C 83.54, H 8.51; found C 83.52, H 8.56.

3,3′′-Di-*tert*-butyl-2,2′′-dihydroxy[1,1′;4′,1′′]terphenyl (1): A solution of BBr_3 (1 M in CH_2Cl_2, 13 mL, 13 mmol) was added to a solution of **8** (2.06 g, 5.12 mmol) in CH_2Cl_2 (100 mL) at 0 °C. After stirring for 48 h at room temperature, the reaction mixture was quenched by addition of 5% aqueous HCl (100 mL). The aqueous phase was extracted with CH_2Cl_2 (3 × 50 mL). The combined organic phase was washed with brine (50 mL) and dried ($MgSO_4$). Column chromatography (alumina; pentane/CH_2Cl_2, 9:1) afforded **1** (1.73 g) as a colorless solid. Yield: 90%. M.p. 163–165 °C. ^{1}H NMR (500 MHz, $CDCl_3$): δ = 7.60 (s, 4 H, 2′-H, 3′-H, 5′-H and 6′-H), 7.34 (dd, $^3J_{H,H}$ = 7.6 Hz, 2 H, 4,4′′-H), 7.13 (dd, $^3J_{H,H}$ = 7.6 Hz, $^4J_{H,H}$ = 1.4 Hz, 2 H, 6,6′′-H), 6.97 (t, $^3J_{H,H}$ = 7.6 Hz, 2 H, 5,5′′-H), 5.44 (s, 2 H, OH), 1.47 (s, 18 H, *t*Bu-H) ppm. ^{13}C NMR (125 MHz, $CDCl_3$): δ = 151.2, 137.2, 136.6, 130.8, 128.3, 128.1, 127.1, 120.3, 35.1, 29.8 ppm. $C_{26}H_{30}O_2$ (374.52): calcd. C 83.38, H 8.07; found C 83.23, H 8.64.

2-*tert*-Butylanisole (9): A solution of **4** (30.8 mL, 0.2 mol) in THF (50 mL) was slowly added to a suspension of freshly powdered KOH (30.2 g, 0.7 mol) in THF (100 mL) while keeping the temperature <10 °C, and the resulting mixture was stirred for 2 h at room temperature. Subsequently, CH_3I (37.3 mL, 0.6 mmol) was added dropwise at 0 °C, and the reaction mixture stirred overnight at room temperature. The reaction mixture was clarified by filtration, and the filtrate was concentrated. The liquid residue was distilled from sodium to afford **9** (32.5 g). Yield: 99%. ^{1}H NMR (500 MHz, [D$_6$]acetone): δ = 7.33 (dd, $^4J_{H,H}$ = 1.7 Hz, $^3J_{H,H}$ = 7.7 Hz, 1 H), 7.25–7.21 (m, 2 H), 6.96–6.91 (m, 1 H), 3.88 (s, 3 H), 1.43 (s, 9 H) ppm. ^{13}C NMR (125 MHz, $CDCl_3$): δ = 159.0, 138.7, 127.5, 127.0, 120.8, 112.0, 55.4, 35.3, 30.2 ppm.

3-*tert*-Butyl-2-methoxyphenylboronic Acid (10): Anisole **9** (9 mL, 51 mmol) was added to the colorless suspension formed by the reaction of *n*BuLi (2.5 M in hexane, 30 mL, 75 mmol) with TMEDA (5.67 mL, 37.6 mmol) at 0 °C. The resulting mixture was stirred at 0 °C for 30 min then overnight at room temperature. After dilution with THF (45 mL) and cooling down to –78 °C, a solution of triisopropylborate (23.2 mL, 100 mmol) in THF (20 mL) was added dropwise to the reaction mixture. Stirring was continued for 1 h at –78 °C then overnight at room temperature. The reaction was quenched by addition of a 5% aqueous solution of HCl (50 mL), and the product was extracted with CH_2Cl_2 (5 × 50 mL) and dried ($MgSO_4$). Column chromatography (alumina, 0–10% CH_3OH in CH_2Cl_2), followed by washing of the solid residue with cold pentane, afforded boronic acid **10** (6.95 g). Yield: 65%. M.p. 79–80 °C. ^{1}H NMR (500 MHz, $CDCl_3$): δ = 7.67 (dd, $^3J_{H,H}$ = 7.5 Hz, $^4J_{H,H}$ = 1.7 Hz, 1 H, 4-H or 6-H), 7.46 (dd, $^3J_{H,H}$ = 7.5 Hz, $^4J_{H,H}$ = 1.7 Hz, 1 H, 6-H or 4-H), 7.11 (t, $^3J_{H,H}$ = 7.5 Hz, 1 H, 5-H), 6.07 (s, 2 H, OH), 3.82 (s, 3 H, OCH_3), 1.41 (s, 9 H, *t*Bu-H) ppm. ^{13}C NMR (125 MHz, $CDCl_3$): δ = 165.7, 142.1, 134.6, 131.0, 124.2, 64.5, 35.1, 31.3 ppm. $C_{11}H_{17}BO_3$ (208.06): calcd. C 63.50, H 8.24; found C 63.56, H 8.22.

3,3′′-Di-*tert*-butyl-2,2′′-dimethoxy[1,1′;3′,1′′]terphenyl (13): $[Pd(PPh_3)_4]$ (0.087 g, 0.0753 mmol) and K_2CO_3 (1.55 g, 11.25 mmol) were added to a solution of **10** (1.15 g, 5.5 mmol) and 1,3-dibromobenzene (0.3 mL, 2.5 mmol). The reaction mixture was stirred vigorously at 100 °C for 72 h. An extra portion of boronic acid (0.43 g, 2.0 mmol) was added, and the reaction was allowed to proceed for an additional 24 h. Column chromatography (silica; heptane/CH_2Cl_2, 9:1; then alumina, heptane) allowed to separate colorless compounds **12** as an oil (0.088 g) and **13** as a solid (0.593 g). Data for **12**: Yield: 11%. ^{1}H NMR (500 MHz, $CDCl_3$): δ = 7.73 (s, 1 H, 2′-H), 7.51 (d, $^3J_{H,H}$ = 7.8 Hz, 1 H, 6′-H), 7.47 (dd, $^3J_{H,H}$ = 7.8 Hz, $^4J_{H,H}$ = 1.9 Hz, 1 H, 4′-H), 7.33 (d, $^3J_{H,H}$ = 7.7 Hz, 1 H, 6-H), 7.29 (t, $^3J_{H,H}$ = 7.8 Hz, 1 H, 5′-H), 7.15 (d, $^3J_{H,H}$ = 7.7 Hz, 1 H, 4-H), 7.08 (t, $^3J_{H,H}$ = 7.7 Hz, 1 H, 5-H), 3.31 (s, 3 H, OCH_3), 1.44 (s, 9 H, *t*Bu-H) ppm. ^{13}C NMR (125 MHz, $CDCl_3$): δ = 157.6, 143.4, 142.2, 134.0, 132.0, 130.1, 129.7, 127.9, 126.9, 123.5, 122.6, 60.8, 35.3, 31.0 ppm. $C_{17}H_{19}BrO$ (319.24): calcd. C 63.96, H 6.00; found C 63.89, H 6.40. Data for **13**: Yield: 59%. M.p. 114–115 °C. ^{1}H NMR (500 MHz, $CDCl_3$): δ = 7.79 (s, 1 H, 2′-H), 7.55 (dd, $^3J_{H,H}$ = 7.6 Hz, $^4J_{H,H}$ = 1.7 Hz, 2 H, 4′-H

and 6′-H), 7.48 (t, $^3J_{H,H}$ = 7.6 Hz, 1 H, 5′-H), 7.34 (dd, $^3J_{H,H}$ = 7.6 Hz, $^4J_{H,H}$ = 1.6 Hz, 2 H, 4,4′′-H), 7.24 (dd, $^3J_{H,H}$ = 7.6 Hz, $^4J_{H,H}$ = 1.6 Hz, 2 H, 6,6′′-H), 7.15 (t, $^3J_{H,H}$ = 7.6 Hz, 2 H, 5,5′′), 3.36 (s, 6 H, OCH_3), 1.45 (s, 18 H, *t*Bu-H) ppm. ^{13}C NMR (125 MHz, $CDCl_3$): δ = 157.7, 143.2, 140.3, 135.4, 130.0, 129.8, 128.7, 127.8, 126.4, 123.3, 60.5, 35.3, 31.0 ppm. $C_{28}H_{34}O_2$ (402.576): calcd. C 83.54, H 8.51; found C 83.77, H 8.50.

3,3′′-Di-*tert*-butyl-2,2′′-dihydroxy[1,1′;3′,1′′]terphenyl (2): A solution of BBr_3 (0.1 M in CH_2Cl_2, 8 mL, 0.8 mmol) was added to a solution of **13** (0.108 g, 0.268 mmol) in CH_2Cl_2 (10 mL) at –78 °C. After stirring for 1.5 h at this temperature, the reaction mixture was warmed to room temperature. After 5 h stirring the reaction was quenched by addition of 5% aqueous HCl (10 mL). The aqueous phase was extracted with CH_2Cl_2 (3 × 10 mL). The combined organic phase was washed with brine (10 mL) and dried ($MgSO_4$), and the solvent was evaporated. Column chromatography of the residue (silica, 0–20% heptane in CH_2Cl_2) afforded diphenol **2** as a colorless solid (0.052 g). Yield: 52%. M.p. 105–108 °C. ^1H NMR (500 MHz, $CDCl_3$): δ = 7.64 (t, $^3J_{H,H}$ = 7.5 Hz, 1 H, 5′-H), 7.60 (t, $^4J_{H,H}$ = 1.6 Hz, 1 H, 2′-H), 7.54 (dd, $^3J_{H,H}$ = 7.5 Hz, $^4J_{H,H}$ = 1.6 Hz, 2 H, 4′-H and 6′-H), 7.35 (dd, $^3J_{H,H}$ = 7.7 Hz, $^4J_{H,H}$ = 1.6 Hz, 2 H, 4,4′′-H), 7.15 (dd, $^3J_{H,H}$ = 7.7 Hz, $^4J_{H,H}$ = 1.6 Hz, 2 H, 6,6′′-H), 6.97 (t, $^3J_{H,H}$ = 7.7 Hz, 2 H, 5,5′′-H), 5.48 (s, 2 H, OH), 1.48 (s, 18 H, *t*Bu-H) ppm. ^{13}C NMR (125 MHz, $CDCl_3$): δ = 151.1, 138.9, 136.7, 130.9, 130.5, 129.1, 128.4, 128.2, 127.1, 120.3, 35.1, 29.8 ppm. $C_{26}H_{30}O_2 \cdot H_2O$ (392.54): calcd. C 79.56, H 8.22; found C 80.08, H 7.89.

2′-Bromo-3-*tert*-butyl-2-methoxybiphenyl (15): $[Pd(PPh_3)_4]$ (0.034 g, 0.0294 mmol) and a solution of K_2CO_3 (0.622 g, 4.5 mmol) in water (1.5 mL) were added to a solution of boronic acid **10** (0.836 g, 4 mmol) and 1,2-dibromobenzene (**14**; 0.13 mL, 1.08 mmol) in DME (15 mL). The reaction mixture was heated at reflux for 60 h under vigorous stirring. The solvents were evaporated, and the residue was purified by column chromatography (alumina; heptane/CH_2Cl_2, 9:1) to afford **15** (0.340 g) as a colorless oil. Yield: 98%. ^1H NMR (500 MHz, $CDCl_3$): δ = 7.76 (dd, $^3J_{H,H}$ = 7.8 Hz, $^4J_{H,H}$ = 1.1 Hz, 1 H, 3′-H), 7.47 (dd, $^3J_{H,H}$ = 7.8 Hz, $^4J_{H,H}$ = 1.7 Hz, 1 H, 6′-H), 7.44 (dd, $^3J_{H,H}$ = 7.5 Hz, $^4J_{H,H}$ = 2.0 Hz, 1 H, 6-H), 7.41 (td, $^3J_{H,H}$ = 7.8 Hz, $^4J_{H,H}$ = 1.1 Hz, 1 H, 5′-H), 7.26 (td, $^3J_{H,H}$ = 7.8 Hz, $^4J_{H,H}$ = 1.7 Hz, 1 H, 4′-H), 7.18 (dd, $^3J_{H,H}$ = 7.5 Hz, $^4J_{H,H}$ = 2.0 Hz, 1 H, 4-H), 7.14 (t, $^3J_{H,H}$ = 7.5 Hz, 1 H, 5-H), 3.35 (s, 3 H, OCH_3), 1.52 (s, 9 H, *t*Bu-H) ppm. ^{13}C NMR (125 MHz, $CDCl_3$): δ = 157.6, 142.8, 140.8, 134.6, 133.1, 132.1, 130.3, 128.8, 127.3, 126.8, 125.6, 124.0, 122.6, 122.3, 60.4, 35.2, 30.8 ppm. $C_{17}H_{19}BrO$ (319.24): calcd. C 63.96, H 6.00; found C 62.72, H 6.33.

3,3′′-Di-*tert*-butyl-2,2′′-dimethoxy[1,1′;2′,1′′]terphenyl (16)

Method A: $[Pd(PPh_3)_4]$ (0.043 g, 0.0372 mmol) and K_2CO_3 (0.310 g, 2.25 mmol) were added to a solution of **15** (0.120 g, 0.376 mmol) and boronic acid **10** (0.313 g, 1.5 mmol) in DMF (8 mL). The reaction mixture was stirred vigorously at 100 °C for 16 h. The solvent was removed in vacuo. Column chromatography of the residue (alumina, heptane) afforded **16** (0.147 g) as a colorless solid in 97% yield.

Method B: $[Pd(PPh_3)_4]$ (0.070 g, 0.0606 mmol) and K_2CO_3 (1.66 g, 12.0 mmol) were added to a solution of 1,2-dibromobenzene (**14**; 0.49 g, 2.0 mmol) and boronic acid **10** (1.704 g, 8.15 mmol) in DMF (18 mL). The reaction mixture was stirred vigorously at 100 °C for 6 h. After addition of an extra portion of **14** (0.1 mL, 0.83 mmol), the reaction mixture was stirred overnight at 100 °C and the solvent was evaporated. Column chromatography (alumina, heptane) of the residue afforded **16** (0.729 g) in 64% yield. M.p. 119–120 °C. ^1H NMR (500 MHz, $C_2D_2Cl_4$, 410 K): δ = 7.51 (2d, 4 H, 3′,6′-H and 4′,5′-H), 7.14 (dd, $^3J_{H,H}$ = 7.6 Hz, $^4J_{H,H}$ = 1.2 Hz, 2 H, 4,4′′-H or 6,6′′-H), 7.06 (br. d, $^3J_{H,H}$ = 7.6 Hz, 2 H, 6,6′′-H or 4,4′′-H), 6.90 (t, $^3J_{H,H}$ = 7.6 Hz, 2 H, 5,5′′-H), 3.27 (s, 6 H, OCH_3), 1.24 (s, 18 H, *t*Bu-H) ppm. Data for **16**-*anti*: ^1H NMR (500 MHz, $C_2D_2Cl_4$, 275 K): δ = 7.47 (AB of AA′BB′, 2 H, 3′,6′-H), 7.43 (A′B′ of AA′BB′, 2 H, 4′,5′-H), 7.17 (dd, $^3J_{H,H}$ = 7.6 Hz, $^4J_{H,H}$ = 1.6 Hz, 2 H, 6,6′′-H), 7.04 (dd, $^3J_{H,H}$ = 7.6 Hz, $^4J_{H,H}$ = 1.6 Hz, 2 H, 4,4′′-H), 6.90 (t, $^3J_{H,H}$ = 7.6 Hz, 2 H, 5,5′′-H), 3.07 (s, 6 H, OCH_3), 1.05 (s, 18 H, *t*Bu-H) ppm. ^1H NMR (600 MHz, CD_2Cl_2, 240 K): δ = 7.44 (AA′BB′, 4 H, 3′,6′-H and 4′,5′-H), 7.15 (dd, $^3J_{H,H}$ = 7.8 Hz, $^4J_{H,H}$ = 1.8 Hz, 2 H, 4,4′′-H), 7.04 (dd, $^3J_{H,H}$ = 7.8 Hz, $^4J_{H,H}$ = 1.8 Hz, 6,6′′-H), 6.88 (t, $^3J_{H,H}$ = 7.8 Hz, 2 H, 5,5′′-H), 3.06 (s, 6 H, OCH_3), 1.05 (s, 18 H, *t*Bu-H) ppm. ^{13}C NMR (126 MHz, $C_2D_2Cl_4$, 278.5 K): δ = 156.9 (2,2′′-C), 141.3 (3,3′′-C), 139.7 (1′,2′-C), 135.0 (1,1′′-C), 130.4 (3′,6′-C), 130.3 (6,6′′-C), 127.5 (4′,5′-C), 125.6 (4,4′′-C), 122.1 (5,5′′-C), 60.0 (OCH_3), 34.6 [$C(CH_3)_3$], 30.5 [$C(CH_3)_3$] ppm. Data for **16**-*syn*: ^1H NMR (500 MHz, $C_2D_2Cl_4$, 275 K): δ = 7.67 (dd, $J_{H,H}$ = 5.6 Hz, $J_{H,H}$ = 3.4 Hz, 2 H, 3′,6′-H), 7.42 (dd, $J_{H,H}$ = 5.6 Hz, $J_{H,H}$ = 3.4 Hz, 2 H, 4′,5′-H), 7.09 (d, $^3J_{H,H}$ = 7.6 Hz, 2 H, 4,4′′-H), 6.76 (t, $^3J_{H,H}$ = 7.6 Hz, 2 H, 5,5′′-H), 6.65 (d, $^3J_{H,H}$ = 7.6 Hz, 2 H, 6,6′′-H), 3.36 (s, 6 H, OCH_3), 1.19 (s, 18 H, *t*Bu-H) ppm. ^1H NMR (600 MHz, CD_2Cl_2, 240 K): δ = 7.63 (d, $J_{H,H}$ = 5.7 Hz, $J_{H,H}$ = 3.3 Hz, 2 H, 3′,6′-H), 7.40 (dd, $J_{H,H}$ = 5.7 Hz, $J_{H,H}$ = 3.3 Hz, 2 H, 4′,5′-H), 7.07 (dd, $^3J_{H,H}$ = 8.0 Hz, $^4J_{H,H}$ = 1.5 Hz, 4,4′′-H), 6.74 (t, $^3J_{H,H}$ = 8.0 Hz, 2 H, 5,5′′-H), 6.63 (dd, $^3J_{H,H}$ = 8.0 Hz, $^4J_{H,H}$ = 1.5 Hz, 2 H, 6,6′′-H), 3.32 (s, 6 H, OCH_3), 1.16 (s, 18 H, *t*Bu-H) ppm. ^{13}C NMR (126 MHz, $C_2D_2Cl_4$, 278.5 K): δ = 157.4 (2,2′′-C), 142.7 (3,3′′-C), 138.7 (1′,2′-C), 134.5 (1,1′′-C), 130.8 (3′,6′-C), 130.5 (6,6′′-C), 127.3 (4′,5′-C), 125.6 (4,4′′-C), 122.3 (5,5′′-C), 60.3 (OCH_3), 34.9 [$C(CH_3)_3$], 30.6 [$C(CH_3)_3$] ppm. $C_{28}H_{34}O_2$ (402.576): calcd. C 83.54, H 8.51; found C 83.26, H 8.30.

3,3′′-Di-*tert*-butyl-2,2′′-dihydroxy[1,1′;2′,1′′]terphenyl (3): A solution of BBr_3 (0.1 M in CH_2Cl_2, 8 mL, 0.8 mmol) was added to a solution of **16** (0.108 g, 0.268 mmol) in CH_2Cl_2 (10 mL) at –78 °C. After 1.5 h stirring at this temperature, the reaction mixture was warmed to room temperature and further stirred for 24 h. The reaction was quenched with 5% aqueous HCl (10 mL). The aqueous phase was extracted with CH_2Cl_2 (3 × 10 mL). The combined organic extract was washed with brine (10 mL) and dried ($MgSO_4$), and the solvents were evaporated. Column chromatography of the residue (silica; heptane/CH_2Cl_2, 8:2) afforded diphenol **3** (0.078 g) as a pale-yellow solid. Yield: 78%. M.p. 128–132 °C. ^1H NMR (500 MHz, $C_2D_2Cl_4$, 400 K): δ = 7.57 (br. s, 4 H, 3′,6′-H and 4′,5′-H), 7.15 (d, $^3J_{H,H}$ = 7.6 Hz, 2 H, 4,4′′-H or 6,6′′-H), 7.06 (d, $^3J_{H,H}$ = 7.6 Hz, 2 H, 6,6′′-H or 4,4′′-H), 6.76 (t, $^3J_{H,H}$ = 7.6 Hz, 2 H, 5,5′′-H), 4.87 (br. s, 2 H, OH), 1.33 (s, 18 H, *t*Bu-H) ppm. Data for **3**-*anti*: ^1H NMR (500 MHz, $C_2D_2Cl_4$, 240 K): δ = 7.56 (AB of AA′BB′, 2 H, 3′,6′-H), 7.50 (A′B′ of AA′BB′, 2 H, 4′,5′-H), 7.08 (dd, $^3J_{H,H}$ = 7.5 Hz, $^4J_{H,H}$ = 1.5 Hz, 2 H, 4,4′′-H), 6.96 (dd, $^3J_{H,H}$ = 7.5 Hz, $^4J_{H,H}$ = 1.5 Hz, 2 H, 6,6′′-H), 6.77 (t, $^3J_{H,H}$ = 7.5 Hz, 2 H, 5,5′′-H), 4.83 (s, 2 H, OH), 1.12 (s, 18 H, *t*Bu-H) ppm. ^1H NMR (600 MHz, CD_2Cl_2, 240 K): δ = 7.56 (AB of AA′BB′, 2 H, 3′,6′-H), 7.50 (A′B′ of AA′BB′, 2 H, 4′,5′-H), 7.08 (dd, $^3J_{H,H}$ = 7.5 Hz, $^4J_{H,H}$ = 1.5 Hz, 2 H, 4,4′′-H), 6.93 (dd, $^3J_{H,H}$ = 7.5 Hz, $^4J_{H,H}$ = 1.5 Hz, 2 H, 6,6′′-H), 6.68 (t, $^3J_{H,H}$ = 7.5 Hz, 2 H, 5,5′′-H), 4.95 (s, 2 H, OH), 1.16 (s, 2 H, *t*Bu-H) ppm. ^{13}C NMR (151 MHz, $C_2D_2Cl_4$, 273 K): δ = 152.2 (2,2′′-C), 138.8 (1′,2′-C), 137.6 (3,3′′-C), 133.5 (4′,5′-C), 131.1 (3′,6′-C), 129.3 (6,6′′-C), 129.2 (1,1′′-C), 128.3 (4,4′′-C), 121.5 (5,5′′-C), 36.1 ($C(CH_3)_3$), 31.0 ($C(CH_3)_3$) ppm. Data for **3**-*syn*: ^1H NMR (500 MHz, $C_2D_2Cl_4$, 240 K): δ = 7.53 (s, 4 H, 3′,4′,5′,6′-H), 7.06 (dd, $^3J_{H,H}$ = 7.5 Hz,

$^4J_{H,H}$ = 1.5 Hz, 2 H, 4,4′′-H), 6.75 (dd, $^3J_{H,H}$ = 7.5 Hz, $^4J_{H,H}$ = 1.5 Hz, 2 H, 6,6′′-H), 6.66 (t, $^3J_{H,H}$ = 7.5 Hz, 2 H, 5,5′′-H), 5.23 (br. s, 2 H, OH), 1.20 (s, 18 H, *t*Bu-H) ppm. ^{1}H NMR (600 MHz, CD_2Cl_2, 240 K): δ = 7.54 (AB of AA′BB′, 2 H, 3′,6′-H), 7.50 (A′B′ of AA′BB′, 2 H, 4′,5′-H), 7.07 (dd, $^3J_{H,H}$ = 7.5 Hz, $^4J_{H,H}$ = 1.5 Hz, 2 H, 4,4′′-H), 6.77 (dd, $^3J_{H,H}$ = 7.5 Hz, $^4J_{H,H}$ = 1.5 Hz, 2 H, 6,6′′-H), 6.66 (t, $^3J_{H,H}$ = 7.5 Hz, 5,5′′-H), 5.24 (s, 2 H, OH), 1.22 (s, 18 H, *t*Bu-H) ppm. ^{13}C NMR (151 MHz, $C_2D_2Cl_4$, 273 K): δ = 152.4 (2,2′′-C), 139.0 (1′,2′-C), 137.5 (3,3′′-C), 133.1 (4′,5′-C), 130.7 (3′,6′-C), 130.4 (6,6′′-C), 129.2 (1,1′′-C), 127.7 (4,4′′-C), 121.1 (5,5′′-C), 36.1 [*C*(CH_3)$_3$], 31.2 [C(*C*H$_3$)$_3$] ppm. $C_{26}H_{30}O_2$ (374.522): calcd. C 83.38, H 8.07; found C 82.57, H 8.13.

X-ray Diffraction: Single crystals of **16** were grown by slow evaporation of dichloromethane solutions. Compound **16** crystallizes in the triclinic system (space group $P\bar{1}$) with two molecules per unit cell (Z = 2). Unit cell parameters at T = 115(2) K are: a = 7.5365(1) Å, b = 11.1804(2) Å, c = 14.8713(2) Å, α = 94.399(1)°, β = 98.277(1)°, γ = 106.750(1)°. A colorless single-crystal specimen of prismatic shape ($0.30 \times 0.25 \times 0.20$ mm^3) was selected for the X-ray diffraction experiment at T = 115(2) K. The X-ray source was graphite monochromated Mo-K_α radiation (λ = 0.71073 Å) from a sealed tube. Data were collected with a Nonius Kappa CCD diffractometer, equipped with a nitrogen jet stream low-temperature system (Oxford Cryosystems), and using the COLLECT software.[14] Lattice parameters were obtained by a least-squares fit to the optimized setting angles of 9577 collected reflections in the full theta range data collection $1.39 < \theta < 27.56°$. Intensity data were recorded as ϕ and ω-scans with κ offsets. Data reduction was done using DENZO software,[15] and did not require absorption corrections. The structure was solved by direct methods by using the SIR92 program.[16] Refinements were carried out by full-matrix least-squares on F^2 by using the SHELXL-97 program[17] and the complete set of reflections. Anisotropic thermal parameters were used for non-H atoms. Hydrogen atoms were refined with a global isotropic thermal factor and placed at calculated positions using a riding model (all of them were located in the Fourier synthesis). The structure was converged to the final statistical agreement factors (R_1 = 0.0382 and 0.0469 for $I > 2\sigma(I)$ and all data, respectively). Crystal data, collection and refinement details are given in Table S5 (Supporting Information). CCDC-739863 (for **16**) contains the supplementary crystallographic data for this paper. These data can be obtained free of charge from The Cambridge Crystallographic Data Centre via www.ccdc.cam.ac.uk/data_request/cif.

Calculations: All calculations were performed in the gas phase, with the Gaussian 03 program package[18] by using density functional theory (DFT) with the hybrid exchange-correlation B3LYP functional.[19] The molecular structures of the conformers of **16** and **3** were optimized starting from the 6-31G(d,p) up to the extended 6-311+G(d,p) basis sets. Frequency calculations were then performed at the same level of theory on each optimized structure in order to check that they correspond to true energy minima and also to compute zero-point energy corrections.

Molecular structures at the transitions states (TS) linking the interconverted conformers were obtained in first approximation by performing relaxed potential energy scans. The scanning coordinates were phenyl–phenyl (τ_1) or phenyl–methoxy (τ_2) torsion angles (Supporting Information, Figure S1). The approximate TS molecular structures were subsequently fully optimized. At the end of the procedure frequency calculations proved the true nature of the TS (only one imaginary frequency).

Supporting Information (see footnote on the first page of this article): Optimized molecular structures of the lowest energy conformations of **16** and **3** and the transition states between them; VT ^{1}H NMR spectra of terphenyl **3**; details of the ^{1}H–^{1}H ROESY NMR spectra of **16** and **3**; crystallographic data.

Acknowledgments

The Conseil Régional de Bourgogne is acknowledged for a postdoctoral fellowship (M.M.G.). The Institut Jean Barriol (Nancy-Université) and GENCI-CINES (Grant 2009-X2009085106) are thanked for providing access to computational facilities. We are grateful to J. Ángyán and F. Hoffmann for help with the theoretical calculations.

[1] a) W. Tang, X. Zhang, *Chem. Rev.* **2003**, *103*, 3029–3069; b) Y. Chen, S. Yekta, A. K. Yudin, *Chem. Rev.* **2003**, *103*, 3155–3211; c) C. Nájera, J. M. Sansano, J. M. Saá, *Eur. J. Org. Chem.* **2009**, 2385–2400.
[2] T. Agapie, J. E. Bercaw, *Organometallics* **2007**, *26*, 2957–2959.
[3] a) S. Sarkar, A. R. Carlson, M. K. Veige, J. M. Falkowski, K. A. Abboud, A. S. Veige, *J. Am. Chem. Soc.* **2008**, *130*, 1116–1117; b) S. Sarkar, K. A. Abboud, A. S. Veige, *J. Am. Chem. Soc.* **2008**, *130*, 16128–16129.
[4] C.-J. F. Du, H. Hart, K.-K. D. Ng, *J. Org. Chem.* **1986**, *51*, 3162–3165.
[5] Y. Zhang, J. Wang, Y. Mu, Z. Shi, C. Lü, Y. Zhang, L. Qiao, S. Feng, *Organometallics* **2003**, *22*, 3877–3883.
[6] N. Miyaura, A. Suzuki, *Chem. Rev.* **1995**, *95*, 2457–2483.
[7] a) D. Zim, A. S. Gruber, G. Ebeling, J. Dupont, A. L. Monteiro, *Org. Lett.* **2000**, *2*, 2881–2884; b) E. J.-G. Anctil, V. Snieckus, *J. Organomet. Chem.* **2002**, *653*, 150–160.
[8] R. B. Bedford, M. E. Limmert, *J. Org. Chem.* **2003**, *68*, 8669–8682.
[9] J. W. Anthis, I. Filippov, D. E. Wigley, *Inorg. Chem.* **2004**, *43*, 716–724.
[10] Y. Hoshino, N. Miyaura, A. Suzuki, *Bull. Chem. Soc. Jpn.* **1988**, *61*, 3008–3010.
[11] One-pot disubstitution has been shown, in fact, to be strongly favored by the use of electron-rich *t*Bu$_3$P: C.-G. Dong, Q.-S. Hu, *J. Am. Chem. Soc.* **2005**, *127*, 10006–10007.
[12] Stereodynamics of *ortho*-terphenyls: a) R. H. Mitchell, J. S.-H. Yan, *Can. J. Chem.* **1980**, *58*, 2584–2587; b) G. Bott, L. D. Field, S. Sternhell, *J. Am. Chem. Soc.* **1980**, *102*, 5618–5626; c) A. Mazzanti, L. Lunazzi, M. Minzoni, J. E. Anderson, *J. Org. Chem.* **2006**, *71*, 5474–5481.
[13] This was determined by solving the equation: $\ln(T_c/\Delta\nu) = (1/RT_c)\Delta G_c^{\ddagger} - 22.96$ for the signals of the *t*Bu protons, taking into account the variation of $\Delta\nu$ with the temperature.
[14] B. Nonius, *COLLECT*, *Data Collection Software*, Delft, The Netherlands, **1998**.
[15] Z. Otwinowski, W. Minor, *Methods Enzymol.* **1997**, *276*, 307–326.
[16] A. Altomare, M. C. Burla, M. Camalli, G. L. Cascarano, C. Giacovazzo, A. Guagliardi, A. G. G. Moliterni, G. Polidori, R. Spagna, *J. Appl. Crystallogr.* **1999**, *32*, 115–119.
[17] G. M Sheldrick, *SHELXL-97*, *Program for the Refinement of Crystal Structures*, University of Göttingen, Göttingen, Germany, **1997**.
[18] M. J. Frisch, G. W. Trucks, H. B. Schlegel, G. E. Scuseria, M. A. Robb, J. R. Cheeseman, J. A. Montgomery Jr., T. Vreven, K. N. Kudin, J. C. Burant, J. M. Millam, S. S. Iyengar, J. Tomasi, V. Barone, B. Mennucci, M. Cossi, G. Scalmani, N. Rega, G. A. Petersson, H. Nakatsuji, M. Hada, M. Ehara, K. Toyota, R. Fukuda, J. Hasegawa, M. Ishida, T. Nakajima, Y. Honda, O. Kitao, H. Nakai, M. Klene, X. Li, J. E. Knox, H. P. Hratchian, J. B. Cross, V. Bakken, C. Adamo, J. Jaramillo, R. Gomperts, R. E. Stratmann, O. Yazyev, A. J. Austin, R. Cammi, C. Pomelli, J. W. Ochterski, P. Y. Ayala, K. Morokuma, G. A. Voth, P. Salvador, J. J. Dannenberg, V. G. Zakrzew-

ski, S. Dapprich, A. D. Daniels, M. C. Strain, O. Farkas, D. K. Malick, A. D. Rabuck, K. Raghavachari, J. B. Foresman, J. V. Ortiz, Q. Cui, A. G. Baboul, S. Clifford, J. Cioslowski, B. B. Stefanov, G. Liu, A. Liashenko, P. Piskorz, I. Komaromi, R. L. Martin, D. J. Fox, T. Keith, M. A. Al-Laham, C. Y. Peng, A. Nanayakkara, M. Challacombe, P. M. W. Gill, B. Johnson, W. Chen, M. W. Wong, C. Gonzalez, J. A. Pople, *Gaussian 03*, revision B.05, Gaussian, Inc., Wallingford, CT, **2004**.

[19] A. D. Becke, *J. Chem. Phys.* **1993**, *98*, 5648–5652.

Received: July 24, 2009
Published Online: November 11, 2009

